Multi-Watt cavity for 266 nm light in vacuum

IOP Publishing *Phys. Scr.* **98** (2023) 085521 https://doi.org/10.1088/1402-4896/ace300

Physica Scripta

OPEN ACCESS

RECEIVED
24 April 2023

REVISED
22 June 2023

ACCEPTED FOR PUBLICATION
29 June 2023

PUBLISHED
20 July 2023

PAPER

Multi-Watt cavity for 266 nm light in vacuum

Christian Brand[1,2], **Christian Knobloch**[1], **Ksenija Simonović**[1] and **Markus Arndt**[1]

[1] University of Vienna, Faculty of Physics, Vienna Doctoral School of Physics & VCQ, Boltzmanngasse 5, A-1090 Vienna, Austria
[2] German Aerospace Center (DLR), Institute of Quantum Technologies, Wilhelm-Runge-Straße 10, D-89081 Ulm, Germany

E-mail: Christian.Brand@dlr.de

Keywords: cavity, UV-radiation, 266 nm, contamination, contamination-resistant

Supplementary material for this article is available online

Abstract

Intense coherent ultraviolet radiation is gaining increasing importance in advanced quantum technologies—from optical clocks and quantum computers to matter-wave interferometry—as well as in photochemistry, life sciences, semiconductor industry, and space applications. Since the preparation of multi-Watt light sources is still an open challenge for many ultraviolet wavelengths, resonant enhancement in a cavity is an attractive alternative. However, many experiments with atoms, molecules or nanoparticles require isolation in high vacuum where UV optics often show fast degradation. Here, we present stable performance of a cavity for 266 nm light with several Watt of intra-cavity power in high vacuum despite the presence of hydrocarbons. Comparing two sets of cavity mirrors indicates that this feat is connected to the micro-chemical environment at the topmost coating layer. Our study emphasizes the need for further developments in this direction to facilitate robust, compact, and high-performing devices employing UV radiation.

1. Introduction

Laser-induced degradation of optical components in vacuum is a common challenge faced in sealed [1–3] and space-based laser systems [4–8], lithography [9–12], spectroscopy [13–18], and quantum optics [19–22]. Often this can be traced back to residual hydrocarbons that photochemically react with the optical components and deteriorate their properties [3, 4, 23]. The preferential binding sites of the contamination are Si-OH groups or defects originating from strained Si-O bonds [3, 23, 24]. Once bound, the molecules can act as starting points for a polymerization reaction [7, 9, 25], leading to the effective deposition of carbon in the irradiated area [3, 9, 23, 26]. The severity of the contamination depends on the partial pressure of the hydrocarbons as well as their chemical composition, resulting in layers with a thickness up to half a micron [23].

An integral part of this process is the chemical micro-environment at the topmost mirror layer. In particular, substrate coating technology has a strong influence on the binding of adducts. Both the porosity and the availability of possible reaction sites on the surface are important [23, 24]. Even catalytic properties of defects have been discussed [26], in line with the observation that coatings with high internal strain are more strongly contaminated than uncoated substrates [6, 27, 28].

While the covalent bonds between the mirror and the contamination prevent thermal cleaning [7], the deposited carbon can be removed by ozone [9, 26, 29], oxygen plasmas [3, 30] or oxygen at a partial pressure above 20 Pa [4, 9, 12, 31], preferentially in the presence of ultraviolet laser radiation. Constantly flushing the optics with oxygen prevents degradation entirely [2, 18] and high power UV-cavities in a segmented vacuum chamber have been demonstrated [15]. Alternatively, removing organic contamination entirely is a very successful route to ensure long-term stability [11, 32, 33].

These methods require either a very clean system or a highly elaborate and large setup to prevent or undo the degradation of the optics. This becomes an issue as soon as the size is restricted as in space missions or as organic components are to be investigated since they are precursors to contamination on the substrate. For wavelengths around 390 nm, it has been argued that sealing the surface with a layer of SiO_2 can prevent degradation of the optics [19]. However, this finding has been contested by others who reported contamination even for optics with a thick SiO_2 top layer [20].

The discussion is further complicated by the fact that the experiments were performed under a large variety of boundary conditions. These encompass the particulars of the coating process, the pressure regime used, the chemical nature of the hydrocarbons, and so on. Here we compare the performance of two sets of cavity mirrors, both coated for 266 nm, in the same vacuum setup. The mirrors were manufactured by two different companies according to the same specifications and both systems feature a SiO_2 layer on top. Still, their properties vary dramatically. While mirror set (A) degrades on the time scale of seconds as soon as the cavity is operated in pre-vacuum, mirror set (B) retains its properties under all tested conditions ($5 \times 10^{-10} - 0.1$ mbar). Set (B) thus allows us to run a multi-Watt cavity at 266 nm in vacuum in the presence of hydrocarbons without degradation. This strongly suggests that the chemical micro-environment on the mirror surface determines its performance under the tested conditions.

2. Experimental setup

We generate continuous high-power radiation at $\lambda = 266$ nm by frequency-doubling a high-power, single-line DPSS laser beam (Coherent Verdi V10, $P \leqslant 10$ W, $\lambda = 532$ nm, TEM_{00}, FWHM line width $\Delta\nu = 5$ MHz) in an external cavity frequency doubler (Sirah WaveTrain2). We reach an output power of $P_{266} = 1$ W for a fundamental input power of $P_{532} = 3.5$ W and even $P_{266} = 3$ W when pumping with $P_{532} = 8$ W. However, we usually restrict the output to $P_{266} \leqslant 0.5$ W to increase the lifetime of the UV optics. To facilitate the coupling to the cavity in vacuum, the UV beam is shaped using a cylindrical and a spherical telescope as shown in figure 1. The cylindrical telescope consists of the lenses c1 ($f = 75$ mm) and c2 ($f = 50$ mm) while the spherical telescope is composed of the lenses s1 ($f = 200$ mm) and s2 ($f = 100$ mm). These are adjusted to realize a Gaussian beam with a $1/e^2$ diameter of 640 ± 20 μm at the position of the plan-convex coupling lens CL ($f = 250$ mm). Coupling into the cavity is optimized using two bending mirrors (not shown) behind the coupling lens. The light reflected by the cavity is registered with a suitable photodetector Det1 (Thorlabs DET25K/M).

The cavity consists of two spherical mirrors produced by ion beam sputtering. They have a radius of curvature of $r = 100$ mm and a nominal reflectivity of $R = (98.75 \pm 0.25)\%$. The high-reflective mirror surfaces are separated by $L_c = 3.34$ mm, resulting in a free-spectral range of $\nu_{\mathrm{FSR}} = 44.9$ GHz and a cavity waist of $w_0 = 33$ μm in the center and only 0.3 μm larger on the mirror [34, 35]. Given a finesse of $F = 250$, the line width amounts to $\Delta\nu_{1/2} = 180$ MHz (FWHM), which is more than one order of magnitude larger than the one of the pump laser. The cavity length can be adjusted using a ring piezo (Piezomechanik HPCh 150/10-5/3), which carries the cavity mirror M2. The impedance matching and coupling efficiency of the light to the cavity are estimated by scanning over the cavity resonance and monitoring the amount of the reflected light. To record the cavity spectrum, 10% of the transmitted light is guided by the beam splitter BS to the photo-detector Det2 (Thorlabs PDA10A2). The reading from this detector is also used to lock the cavity to the incident beam via a side-of-fringe locking scheme. Here, we typically set the lock to $50 - 75\%$ of the peak intensity of the TEM_{00} mode. The intensity inside the cavity is calculated from the power detected with the power meter PM (Coherent PowerMax USB PM 150-50C) behind the cavity, the enhancement factor $F/\pi \approx 80$, and the power reduction due to the beam splitter (10%).

The cavity is mounted in a simple aluminum frame and placed in a UHV-compatible vacuum chamber. A turbo molecular pump (700 l/s) backed by a rotary vane pump together with a cold baffle (77 K) can reduce the pressure at room temperature to below 5×10^{-10} mbar. The main sources of contamination originate from the rotary vane pump and several Viton rings. The latter are used to seal the two entrance windows of the chamber, damp vibrations of the cavity, and preload the ring piezo.

3. Results

3.1. Performance of set (A)

We start with characterizing the cavity mirror set (A). At ambient pressure, these mirrors show the desired behavior: Once optimized, the cavity spectrum remains stable and does not degrade over time. This allows for locking the cavity with several Watt of intra-cavity power for more than an hour in air, as shown in the Supplementary Material. Comparing the cavity spectrum before and after locking shows no signs of degradation either.

The situation changes as soon as we reduce the pressure p. Below a certain threshold, the cavity spectrum decays, leading to a time-dependent decrease in the intensity of the TEM_{00} mode (Supplementary Material). For the current data set, this point is reached around 1–2 mbar. To follow this process, we optimized the mode coupling at a pressure where no degradation takes place, that is, at 10 mbar. Then, we blocked the incoming laser

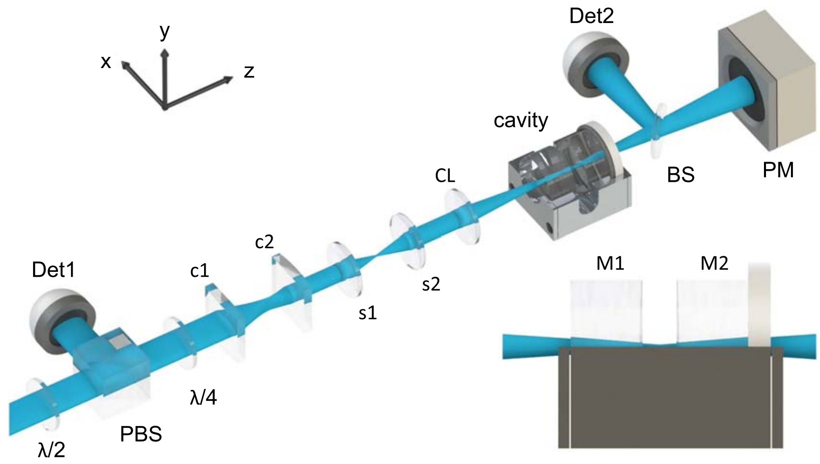

Figure 1. Sketch of the experimental setup. The input power is adjusted with a $\lambda/2$ plate and a polarizing beam splitter (PBS). After passing the optical diode (PBS and $\lambda/4$) the laser is shaped via a cylindrical (c1 & c2) and a spherical telescope (s1 & s2) to reach a Gaussian beam with a $1/e^2$ diameter of 640 ± 20 μm at the position of the coupling lens CL. The cavity itself (M1 & M2) is situated in a vacuum chamber and is shown in the inset. In the drawing, the upper part of the cavity has been removed to facilitate a view inside. To lock the cavity to the incoming laser beam the cavity length is adapted via a ring piezo holding M2. For generating the error signal 10% of the transmitted power is guided by the beam splitter BS to the photo-detector Det2, while the power meter PM measures the intensity of the transmitted light. The reflected light is registered with the detector Det1.

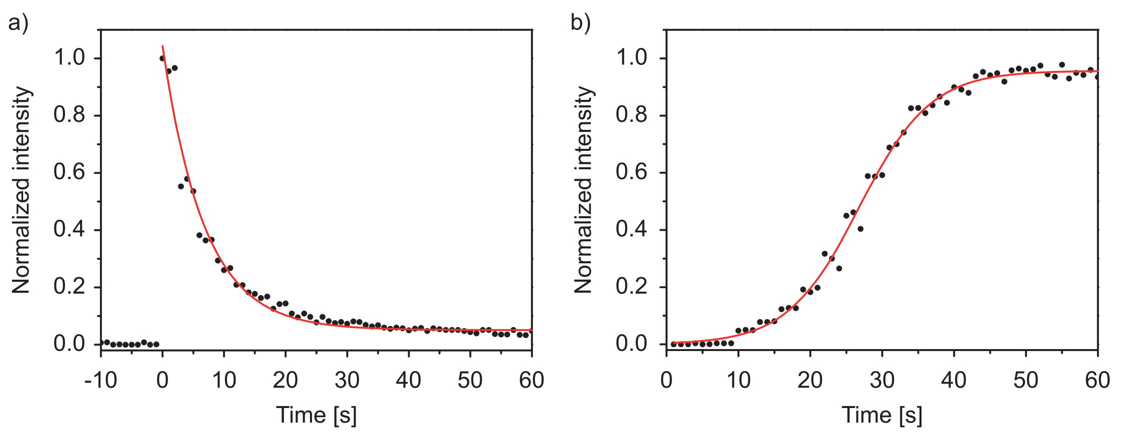

Figure 2. Decay and recovery of the normalized cavity transmission for mirror set (A). (a) As soon as the cavity is pumped with 266 nm light at $p < 1$ mbar, the intensity of the TEM_{00} decays exponentially. For $p = 0.1$ mbar this results in a mean decay lifetime $\tau_{\rm dec}$ of 7.7 ± 0.2 s. (b) In the presence of UV light the cavity transmittance recovers at $p = 8$ mbar with $\tau_{\rm rec} = 5.6 \pm 0.1$ s.

and evacuated the cavity to the target pressure. As soon as we removed the beam dump and exposed the cavity to the UV light, its spectrum started to decay as shown for $p = 0.1$ mbar in figure 2(a)). During the whole procedure, we continuously scanned the cavity with 100 Hz over a large portion of the spectrum (about 40 GHz). Fitting the time-dependent peak value of the TEM_{00} with a single-exponential decay

$$y = y_0 + A \times \exp(-t/\tau_{\rm dec}) \tag{1}$$

yields the amplitude A, the offset y_0, and the mean decay lifetime $\tau_{\rm dec}$, which amounts to 7.7 ± 0.2 s in this run. The degradation can be reversed completely by leaking in laboratory air to increase the pressure above 2 mbar while pumping the cavity with UV light, as shown in figure 2(b). Venting the vacuum chamber with pure nitrogen had no beneficial effect. The time-dependent increase in transmitted power is reproduced well by a logistic function

$$y = y_0 + \frac{A}{1 + \exp(-(t - t_c))/\tau_{\rm rec}}, \tag{2}$$

which allows us to extract the mean recovery time $\tau_{\rm rec}$ and the midpoint t_c. Repeating the cycle of decay and recovery in the pressure range between $0.1 - 22$ mbar shows that these processes approach a threshold at about $1 - 2$ mbar as mentioned before (see figure 3). At this pressure $p_{\rm thresh}$, neither a complete decay nor complete recovery is observed.

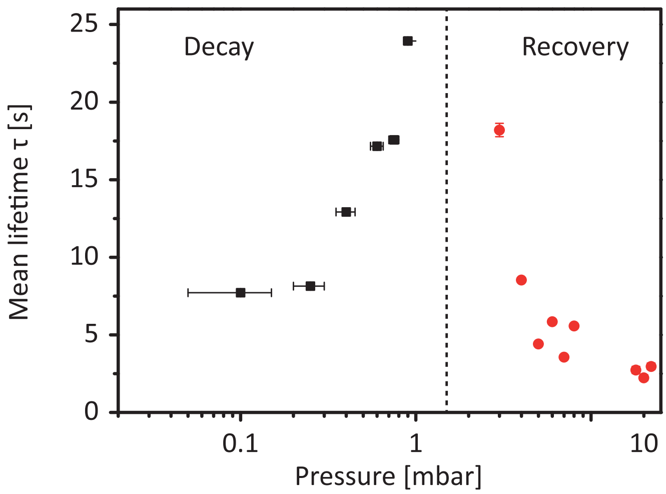

Figure 3. Pressure-dependent lifetimes τ of the cavity transmittance for mirror set (A). For pressures below the estimated threshold at 1.5 mbar (broken line), the cavity spectrum decays over time, while it is recovered for pressures above the threshold.

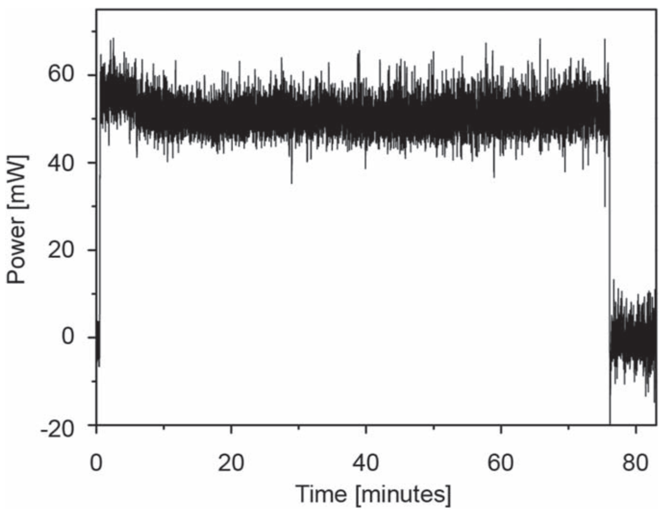

Figure 4. A typical power trace recorded with the power meter PM while keeping the cavity locked in ultra-high vacuum. The cavity remains locked for 75 min with a mean intra-cavity power of 50 mW $\times$ 79.5/0.9 = 4.4 W.

The decay lifetime strongly depends on the cleanliness of the vacuum chamber. After baking and keeping the test setup at 10^{-9} mbar for a few weeks, we repeated the measurement at 0.1 mbar. This led to an increase of τ_{dec} from 7.7 $\pm$ 0.2 s to 195 $\pm$ 3 s, suggesting that p_{thresh} is shifted to lower pressures. To see whether this allows for stable operation of the cavity in UHV, we performed the decay experiment at $p = 5 \times 10^{-10}$ mbar. Although the mean lifetime τ_{dec} was greatly enhanced to 68 $\pm$ 3 minutes, we still observed an exponential decay even under these conditions (Supplementary Material).

In the experiments shown in figure 2 the pump power coupled in was held constant at 40 mW.

3.2. Performance of mirror set (B)

Exchanging mirror set (A) with (B) has a pronounced effect on the behavior of the cavity at low pressures. In contrast to set (A), we do not observe any time-dependent degradation for mirror set (B), when scanning over the cavity spectrum in vacuum. This allows us to stabilize the cavity with several Watt of intra-cavity power, typically at $p = 5 \times 10^{-10}$ mbar. An exemplary run is shown in figure 4: here we locked the cavity with an intra-cavity power of 4.4 W for more than an hour. The highest intra-cavity power we observed was 5.6 W, which remained stable for half an hour. In total, we have accumulated several hours of stable performance at this power without any signs of degradation over a period of two months. Between the runs, the cavity was always kept at a pressure below 10^{-8} mbar and at 300 K.

4. Discussions

In the experiments, mirror set (A) shows typical signs of degradation due to contamination. First, we observe a rather sharp pressure threshold at which the decay of the cavity sets in [36]. Second, oxygen is required for the recovery of the cavity spectrum, as venting the chamber with pure nitrogen has no effect [29]. The partial pressure of oxygen at the threshold in figure 3 is around 20 Pa, as observed before [4, 9, 12, 31]. After extensive cleaning of the setup, p_{thresh} shifts to lower values. This is in agreement with the observation that p_{thresh} is determined by the ratio of the partial pressures of oxygen and the residual hydrocarbons [36]. Thus, reducing the partial pressure of the hydrocarbons allows for reducing the partial pressure of oxygen as well. While this increases the longevity of the mirrors, it cannot prevent their degrading in the presence of UV radiation [4]: Even after baking and pumping to $p = 5 \times 10^{-10}$ mbar, the cavity spectrum is degrading. To mend this, we would have to remove all hydrocarbons from the vacuum setup [11, 32]. However, as the purpose of the cavity is to provide an intense laser grating for matter-wave diffraction of large organic molecules [37, 38], this is not an option. Flushing the mirrors with oxygen has to be discarded as well, as the resulting increase in pressure would induce collisional decoherence of the matter-wave [39].

In our experiments, we observe comparatively short values of τ_{dec} compared to the literature. On the one hand, this might be connected to the composition of the hydrocarbons. In most previous experiments, highly volatile substances such as small aromatics have been used to precisely control the respective partial pressures. As our main source of contamination is pump oil, we expect the hydrocarbons to be large, long-chained molecules. These molecules have been identified to pose a greater threat for contamination in EUV lithography than lighter ones [40]. On the other hand, also the wavelength might play a role. Light at 266 nm is resonant both to electronic transitions in aromatic hydrocarbons and non-bonding oxygen hole center-defects (NBOHC) in strained silica films [6, 25, 41]. Hence, we might excite both the contaminating particles and the possible reaction sites very effectively [6].

The most important question, however, is why the mirrors of set (B) are not degrading over time. As the top layer in both sets is SiO_2, this cannot be explained by the material, alone. Instead, it seems to be related to the micro-chemical environment of the surface. Previous studies have highlighted the effect of Si-OH groups, strained silica bonds, and defects [8, 23, 24, 41, 42]. Especially the latter seems to play a critical role in the creation of reactive hydrocarbons on the silica surface. Doping silica with fluorine has been shown to reduce the number of strained three- and four-membered rings considerably [43, 44]. This can reduce the defect concentration by about one order of magnitude compared to pure samples [45] and significantly increase the lifetime of mirrors in UV cavities [46].

Based on our observations, it seems that this feat can also be achieved without the use of a process gas, as demonstrated by mirror set (B). This insight also gives the recent discussion on protective SiO_2 layers for UV optics [19–21] a new direction where the micro-chemical environment of the coatings was largely ignored. So, the question is not whether SiO_2 helps or not, but which requirements the top layer has to meet to obtain contamination-resistant coatings. The present findings suggest that the answer to this question might be of vital importance to reliably manufacture contamination-resistant coatings for UV wavelengths in a vacuum environment.

5. Conclusion

We tested the performance of two sets of cavity mirrors for 266 nm in vacuum. While these were fabricated to the same specifications and featured SiO_2 on top, they behaved quite differently in the presence of hydrocarbons. Set (A) showed typical signs of contamination, which led to a decay of the cavity spectrum on the order of seconds while scanning over the cavity resonance. Set (B), however, did not show this behavior, which allowed locking the cavity with several Watts of intra-cavity power in vacuum. This required neither a completely clean setup nor flushing the mirrors with oxygen. We attribute this difference in performance to the micro-chemical environment of the topmost coating layer. Our study highlights the need to better characterize the deposited thin films to reliably produce contamination-resistant coatings. This is of high interest for the realization of compact and reliable setups employing intense radiation in the UV.

Acknowledgments

We acknowledge fruitful discussions with Stefan Kuhn, Randolph Pohl, Ferdinand Schmidt-Kaler, Simon Stellmer, Stephan Truppe, Sid Wright, Jonathan Tinsley, and Stephan Hannig. KS acknowledges financial support from FWF through the Vienna Doctoral School in Physics (Project number: HiDHyS).

Data availability statement

The data that support the findings of this study are openly available [47].

ORCID iDs

Christian Brand https://orcid.org/0000-0003-3872-7769
Ksenija Simonović https://orcid.org/0000-0001-7941-7295
Markus Arndt https://orcid.org/0000-0002-9487-4985

References

[1] Boller K, Haelbich R P, Hogrefe H, Jark W and Kunz C 1983 Investigation of carbon contamination of mirror surfaces exposed to synchrotron radiation *Nucl. Instrum. Methods Phys. Res.* **208** 273–9
[2] Bernhardt B *et al* 2012 Vacuum ultraviolet frequency combs generated by a femtosecond enhancement cavity in the visible *Opt. Lett.* **37** 503–5
[3] Yamada K *et al* 1995 Degradation and restoration of dielectric-coated cavity mirrors in the NIJI-IV FEL *Nucl. Instrum. Methods Phys. Res., Sect. A* **358** 392–5
[4] Wernham D, Alves J, Pettazzi F and Tighe A 2010 Laser-induced contamination mitigation on the ALADIN laser for ADM-Aeolus *Laser Damage Symposium XLII: Annual Symposium on Optical Materials for High Power Lasers* vol 7842 *(Boulder, Colorado)* (SPIE)
[5] Alves J, Pettazzi F, Tighe A and Wernham D 2017 Laser-induced contamination control for high-power lasers in space-based LIDAR missions *International Conference on Space OpticsICSO 2010* vol 10565 *(Rhodes Island, Greece)* (SPIE)
[6] Liessmann M, Jensen L, Balasa I, Hunnekuhl M, Büttner A, Weels P, Neumann J and Ristau D 2015 Scaling of laser-induced contamination growth at 266 nm and 355 nm *Laser-Induced Damage in Optical Materials* vol 9632 *(Boulder, Colorado)* (SPIE)
[7] Pereira A, Roussel J F, van Eesbeek M, Guyt J M, Schmeitzky O and Faye D 2003 Study of the UV-enhancement of contamination *IX International Symposium on Materials in a Space Environment (Noordwijk, The Netherlands)* (ESA Publications Division) 231–8
[8] Riede W, Schroeder H, Bataviciute G, Wernham D, Tighe A, Pettazzi F and Alves J 2011 Laser-induced contamination on space optics *SPIE Laser Damage* vol 8190 *(Boulder, Colorado)* (SPIE) (https://doi.org/10.1117/12.899190)
[9] Kunz R R, Liberman V and Downs D K 2000 Experimentation and modeling of organic photocontamination on lithographic optics *J. Vac. Sci. Technol. B* **18** 1306–13
[10] Chen J *et al* 2009 Detection and characterization of carbon contamination on EUV multilayer mirrors *Opt. Express* **17** 16969–79
[11] Grunow P, Klebanoff L, Graham S, Haney S and Clift W M 2003 Rates and mechanisms of optic contamination in the EUV engineering test stand *Microlithography 2003* vol 5037 *(Santa Clara, California)* (SPIE) (https://doi.org/10.1117/12.499359)
[12] Koster N *et al* 2002 Molecular contamination mitigation in EUVL by environmental control *Microelectron. Eng.* **61-62** 65–76
[13] Beyer A *et al* 2017 The Rydberg constant and proton size from atomic hydrogen *Science* **358** 79
[14] Ahmadi M *et al* 2017 Observation of the 1S–2S transition in trapped antihydrogen *Nature* **541** 506–10
[15] Cooper S F, Burkley Z, Brandt A D, Rasor C and Yost D C 2018 Cavity-enhanced deep ultraviolet laser for two-photon cooling of atomic hydrogen *Opt. Lett.* **43** 1375–8
[16] Schäfer R, Schmidtke G, Strahl T, Pfeifer M and Brunner R 2017 EUV data processing methods of the Solar Auto-Calibrating EUV Spectrometers (SolACES) aboard the International Space Station *Adv. Space Res.* **59** 2207–28
[17] BenMoussa A *et al* 2013 On-orbit degradation of solar instruments *Sol. Phys.* **288** 389–434
[18] Altiere E, Miller E R, Hayamizu T, Jones D J, Madison K W and Momose T 2018 High-resolution two-photon spectroscopy of a 5p56p←5p6 transition of xenon *Phys. Rev. A* **97** 012507
[19] Gangloff D *et al* 2015 Preventing and reversing vacuum-induced optical losses in high-finesse tantalum (V) oxide mirror coatings *Opt. Express* **23** 18014–28
[20] Ballance T G, Meyer H M, Kobel P, Ott K, Reichel J and Köhl M 2017 Cavity-induced backaction in Purcell-enhanced photon emission of a single ion in an ultraviolet fiber cavity *Phys. Rev. A* **95** 033812
[21] Gallego J, Alt W, Macha T, Martinez-Dorantes M, Pandey D and Meschede D 2018 Strong Purcell effect on a neutral atom trapped in an open fiber cavity *Phys. Rev. Lett.* **121** 173603
[22] Brandstätter B *et al* 2013 Integrated fiber-mirror ion trap for strong ion-cavity coupling *Rev. Sci. Instrum.* **84** 123104
[23] Becker S, Pereira A, Bouchut P, Geffraye F and Anglade C 2007 Laser-induced contamination of silica coatings in vacuum *Boulder Damage Symposium 38th: Annual Symposium on Optical Materials for High Power Lasers* vol 6403 *(Boulder, Colorado)* (SPIE)
[24] Guéhenneux G, Ph B, Veillerot M, Pereira A and Tovena I 2006 Impact of outgassing organic contamination on laser-induced damage threshold of optics: effect of laser conditioning *Boulder Damage Symposium XXXVII: Annual Symposium on Optical Materials for High Power Lasers* vol 5991 *(Boulder, Colorado)* (SPIE)
[25] Ferreira L F V, Machado I F, Da Silva J P and Branco T J F 2006 Surface photochemistry: benzophenone as a probe for the study of silica and reversed-phase silica surfaces *Photochem. Photobiol. Sci.* **5** 665–73
[26] Riede W, Allenspacher P, Schröder H, Wernham D and Lien Y 2006 Laser-induced hydrocarbon contamination in vacuum *Boulder Damage Symposium XXXVII: Annual Symposium on Optical Materials for High Power Lasers* vol 5991 *(Boulder, Colorado)* (SPIE)
[27] Wagner P, Schröder H and Riede W 2014 In-situ laser-induced contamination monitoring using long-distance microscopy *SPIE Laser Damage* vol 9237 *(Boulder, Colorado)* (SPIE) (https://doi.org/10.1117/12.2066465)
[28] Schröder H, Wagner P, Kokkinos D, Riede W and Tighe A 2013 Laser-induced contamination and its impact on laser damage threshold *SPIE Laser Damage* vol 8885 *(Boulder, Colorado)* (SPIE) (https://doi.org/10.1117/12.2030002)
[29] Pereira A, Quesnel E and Reymermier M 2009 Dynamic measurements of ultraviolet-enhanced silica contamination by photoluminescence-based diagnostic *J. Appl. Phys.* **105** 013109
[30] McKinney W R and Takacs P Z 1982 Plasma discharge cleaning of replica gratings contaminated by synchrotron radiation *Nucl. Instrum. Methods Phys. Res.* **195** 371–4
[31] Alvez B X R 2018 Antihydrogen spectroscopy and fundamental symmetry tests *Thesis* Aarhus University
[32] Schmitz J, Meyer H M and Köhl M 2019 Ultraviolet Fabry-Perot cavity with stable finesse under ultrahigh vacuum conditions *Rev. Sci. Instrum.* **90** 063102

[33] Kondo K, Oka M, Wada H, Fukui T, Umezu N, Tatsuki K and Kubota S 1998 Demonstration of long-term reliability of a 266-nm, continuous-wave, frequency-quadrupled solid-state laser using β-BaB2O4 *Opt. Lett.* **23** 195–7
[34] Hecht E 2018 *Optik* (De Gruyter)
[35] Kogelnik H and Li T 1966 Laser Beams and Resonators *Appl. Opt.* **5** 1550–67
[36] Hippler M, Wagner P, Schroeder H and Riede W 2016 Laser-induced contamination of space borne laser systems: impact of organic contamination and mitigation by oxygen *SPIE Optical Engineering + Applications* vol 9952 *(San Diego, California)* (SPIE) (https://doi.org/10.1117/12.2236897)
[37] Arndt M, Nairz O, Vos-Andreae J, Keller C, van der Zouw G and Zeilinger A 1999 Wave-particle duality of C60 molecules *Nature* **401** 680–2
[38] Kjałka F, Fein Y Y, Pedalino S, Gerlich S and Arndt M 2022 A roadmap for universal high-mass matter-wave interferometry *AVS Quantum Sci.* **4** 020502
[39] Hornberger K, Uttenthaler S, Brezger B, Hackermüller L, Arndt M and Zeilinger A 2003 Collisional Decoherence Observed in Matter Wave Interferometry *Phys. Rev. Lett.* **90** 160401
[40] Garg R, Wüest A, Gullikson E, Bajt S and Denbeaux G 2008 EUV optics contamination studies in presence of selected hydrocarbons *SPIE Advanced Lithography* vol 6921 *(San Jose, California)* (SPIE) (https://doi.org/10.1117/12.772770)
[41] Skuja L, Hirano M, Hosono H and Kajihara K 2005 Defects in oxide glasses *Phys. Status Solidi C* **2** 15–24
[42] Pasquarello A and Car R 1998 Identification of Raman defect lines as signatures of ring structures in vitreous silica *Phys. Rev. Lett.* **80** 5145–7
[43] Hosono H, Mizuguchi M, Skuja L and Ogawa T 1999 Fluorine-doped SiO2 glasses for F2 excimer laser optics: fluorine content and color-center formation *Opt. Lett.* **24** 1549–51
[44] Hosono H, Ikuta Y, Kinoshita T, Kajihara K and Hirano M 2001 Physical disorder and optical properties in the vacuum ultraviolet region of amorphous SiO2 *Phys. Rev. Lett.* **87** 175501
[45] Hosono H, Mizuguchi M, Kawazoe H and Ogawa T 1999 Effects of fluorine dimer excimer laser radiation on the optical transmission and defect formation of various types of synthetic SiO2 glasses *Appl. Phys. Lett.* **74** 2755–7
[46] Burkley Z, de Sousa Borges L, Ohayon B, Golovozon A, Zhang J and Crivelli P 2021 Stable high power deep-uv enhancement cavity in ultra-high vacuum with fluoride coatings *Opt. Express* **29** 27450
[47] Brand C, Knobloch C, Simonovic K and Arndt M 2023 Data for Multi-Watt cavity for 266 nm light in vacuum (https://doi.org/10.17632/y4fs9jt44b.1)